Appendix

Table of Contents

Appendix Table S1. Crystallographic data and refinement

	Thauera sp. K11 CapP SeMet	*Thauera* sp. K11 CapP Native	*E. coli* MS115-1 CapH NTD	*E. coli* MS115-1 CapH CTD	*E. coli* MS115-1 CapH CTD (I99M)
Data collection					
Synchrotron/Beamline	SSRL 9-2	SSRL 9-2	ALS 5.0.2	ALS 5.0.2	APS 24ID-C
Date collected	02/14/2020	02/14/2020	04/25/2021	5/14/21	07/11/21
Resolution (Å)	40-1.6	40-1.35	40-1.02	100-1.75	59-1.26
Wavelength (Å)	0.97892	0.97892	1.00003	1.00004	0.97918
Space Group	$P4_22_12$	$P4_22_12$	$P2_12_12_1$	$P2_1$	$P4_32_12$
Unit Cell Dimensions (a, b, c) Å	95.28, 95.28, 103.95	95.31, 95.31, 104.92	32.38, 39.68, 47.24	44.02, 39.86, 46.26	38.38, 38.38, 59.43
Unit cell Angles (α,β,γ) °	90, 90, 90	90, 90, 90	90, 90, 90	90, 98.73, 90	90, 90, 90
I/σ (last shell)	21.2 (0.9)	18.7 (0.8)	12.5 (2.0)	26.2 (1.1)	21.1 (2.0)
[1]R_{sym} (last shell)	0.082 (2.61)	0.058 (2.884)	0.068 (0.424)	0.059 (0.637)	0.039 (0.732)
[2]R_{meas} (last shell)	0.085 (2.723)	0.06 (3.012)	0.074 (0.516)	0.070 (0.784)	0.043 (0.809)
[3]$CC_{1/2}$ (last shell)	1 (0.529)	0.999 (0.443)	0.997 (0.814)	1 (0.631)	0.999 (0.830)
Completeness (last shell) %	100.0 (99.8)	99.8 (98.1)	80.8 (11.8)	99.5 (98.8)	99.8 (98.3)
Number of reflections	839884	1388162	144010	50378	74958
unique	63659	106052	25495	15936	12610
Multiplicity (last shell)	13.2 (12.4)	13.1 (11.7)	5.6 (3.0)	3.2 (2.8)	5.9 (5.5)
Refinement					
Resolution (Å)	-	40-1.35	30.4-1.02	45.7-1.75	32.2-1.26
No. of reflections	-	105839	25448	15917	12560
working	-	102934	24251	15208	11966
free	-	2905	1197	709	594
[4]R_{work} (last shell) (%)	-	16.21 (42.68)	16.30 (17.77)	20.98 (28.61)	19.13 (22.50)
[4]R_{free} (last shell) (%)	-	16.79 (43.92)	17.64 (17.00)	23.70 (31.23)	21.36 (24.19)
Structure/Stereochemistry					
No. of atoms	-	4741	1166	2531	642
solvent	-	343	87	60	46
ligand	-	0	10	0	0
hydrogen	-	2159	536	1212	297
r.m.s.d. bond lengths (Å)	-	0.008	0.008	0.010	0.011
r.m.s.d. bond angles (°)	-	0.94	0.993	1.000	0.896
Ramachandran favored/allowed (%)	-	98.2%/100%	100%/100%	99.3%/100%	100%/100%
Molprobity score	-	0.82	0.78	0.64	1.31
[5]SBGrid Data Bank ID	865	864	866	867	868
[6]Protein Data Bank ID	-	7T5T	7T5U	7T5W	7T5V

[1]$R_{sym} = \sum\sum_j |I_j - \langle I \rangle| / \sum I_j$, where I_j is the intensity measurement for reflection j and $\langle I \rangle$ is the mean intensity for multiply recorded reflections.

[2]$R_{meas} = \sum_h [\sqrt{(n/(n\text{-}1))}) \sum_j [I_{hj} - \langle I_h \rangle] / \sum_{hj} \langle I_h \rangle$

where I_{hj} is a single intensity measurement for reflection h, $\langle I_h \rangle$ is the average intensity measurement for multiply recorded reflections, and n is the number of observations of reflection h.

[3]$CC_{1/2}$ is the Pearson correlation coefficient between the average measured intensities of two randomly assigned half-sets of the measurements of each unique reflection. $CC_{1/2}$ is considered significant above a value of ~0.15.

[4]$R_{work,\ free} = \sum||F_{obs}| - |F_{calc}||/|F_{obs}|$, where the working and free R-factors are calculated using the working and free reflection sets, respectively.

[5]Diffraction data for each structure have been deposited with the SBGrid Data Bank (https://data.sbgrid.org) with the noted accession codes.
[6]Coordinates and structure factors for each structure have been deposited with the Protein Data Bank (http://www.rcsb.org) with the noted accession codes.

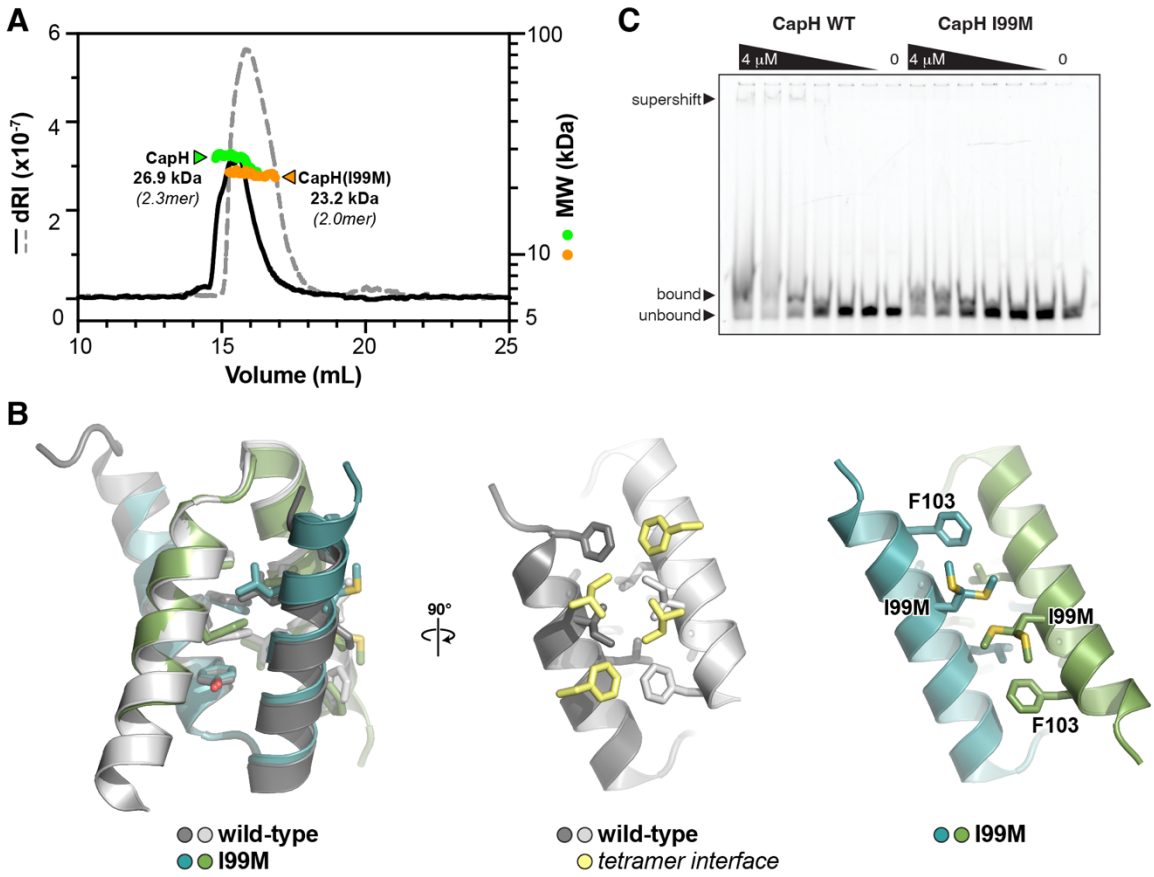

Appendix Figure S1. The CapH I99M mutation disrupts tetramer formation

(A) Size exclusion chromatography coupled to multiangle light scattering chromatogram of CapH and CapH I99M proteins without tags.

(B) *Left:* Cartoon view of the *E. coli* MS115-1 CapH^{CTD} (I99M) structure, with the two protomers colored blue and green. Overlaid is the structure of wild-type CapH^{CTD} (dark gray/light gray). *Center:* Views of the wild-type CapH^{CTD} tetramerization interface, with the dimer shown in dark gray/light gray and interacting residues from the opposite dimer in light yellow. Right: View of the CapH^{CTD} (I99M) tetramerization interface, showing the position of the I99M mutation that disrupts tetramer formation. In the electron density maps, the M99 residues showed partial occupancy for two rotamers, and were modeled with each rotamer at 50% occupancy (both shown as sticks).

(C) Electrophoretic mobility shift of 5'-FAM labeled DNA with a sequence comprised of residues 81-120 of the intergenic region of MS115-1 CBASS after incubation with either wild-type or I99M CapH. Protein concentrations are 4 μM and two-fold dilutions thereof.

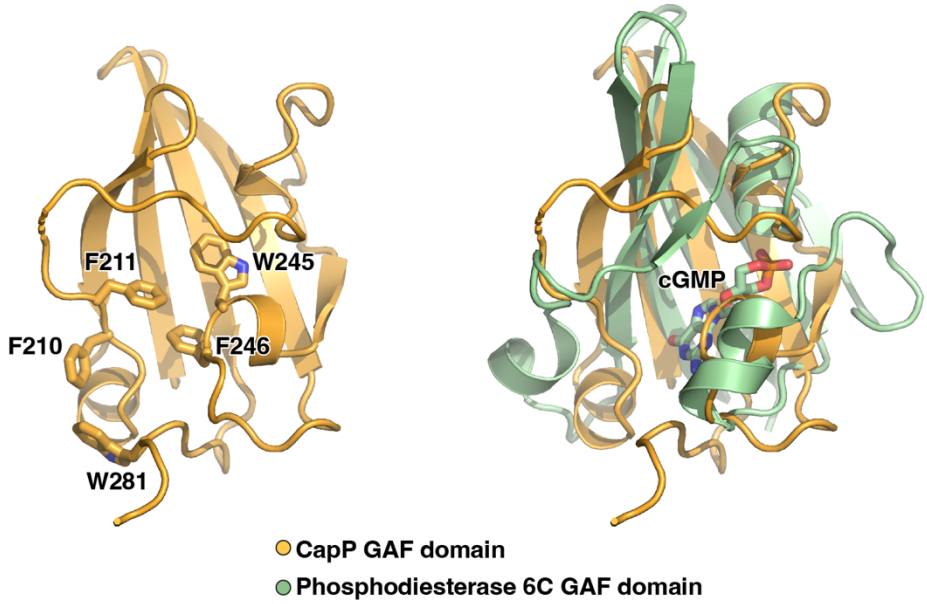

Appendix Figure S2: Structure of the CapP GAF domain

Structural overlay between the *Thauera* sp. K11 CapP GAF domain (orange) and the GAF domain of phosphodiesterase 6C bound to cyclic GMP (green; PDB ID 3DBA; (Martinez et al., 2008)). Surface-exposed aromatic residues potentially involved in CapP-ligand binding are shown as sticks in the left panel.

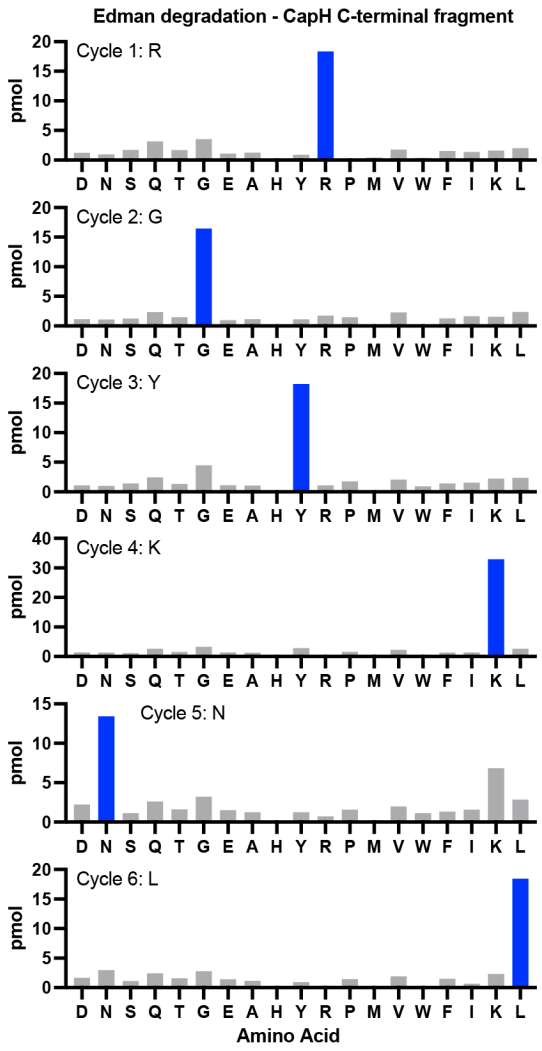

Appendix Figure S3: Edman degradation of CapP cleavage product

Bar graphs showing picomoles (pmol) of each amino acid detected by Edman degradation of the C-terminal cleavage product of MBP-CapH-GFP (denoted by red asterisk in **Figure 5B**). The dominant amino acid for each cycle is shown as a blue bar. The inferred N-terminal sequence (RGYKNL) matches CapH residues 83-88 (see **Figure 5C**).